Effect of Reaction Kinetics of Polymer Electrolyte on the Ion-Conductive Behavior for Poly(oligo oxyethylene methacrylate)–LiTFSI Mixtures

Gun-Ho Kwak, Yoichi Tominaga, Shigeo Asai, Masao Sumita

Department of Chemistry and Materials Science, Tokyo Institute of Technology, 2-12-1 Ookayama, Meguro-Ku, Tokyo 152-8552, Japan

Received 24 June 2002; accepted 21 October 2002

ABSTRACT: The effect of the reaction kinetics on the ionic conductivity for a comblike-type polyether (MEO) electrolyte with lithium bis(trifluoromethane sulfonyl)imide (LiTFSI) was characterized by DSC, complex impedance measurements, and ^{1}H pulse NMR spectroscopy. The ionic conductivity of these electrolytes was affected by the reaction condition of the methacrylate monomer and revealed by the glass transition temperature (T_g), spin–spin relaxation time (T_2), steric effects of the terminal groups, and the number of charge carriers indicated by the VTF kinetic parameter. In this system, the electrolytes prepared by the reaction heating rate of 10°C/min of MEO–H and 15°C/min of MEO–CH_3 showed maximum ionic conductivity, σ_i, two to three times higher in magnitude than that of the σ_i of the others at room temperature. As experimental results, the reaction kinetic rate affected the degree of conversion, the ionic conductivity, and the relaxation behaviors of polyether electrolytes. © 2003 Wiley Periodicals, Inc. J Appl Polym Sci 89: 2149–2156, 2003

Key words: kinetics; conductivity

INTRODUCTION

Since Wright et al. first reported[1] the ionic conduction of poly(ethylene oxide) (PEO) and alkali metal salt complexes in 1973, the ion-transport mechanism and the development of materials have been extensively investigated due to their potential applications such as in high energy density rechargeable batteries, electrochromic display, and ion sensors.[2–5] In this field, the most common approach for high ionic conductivity at operational temperatures has been to add liquid solvents as plasticizers; however, this promotes deterioration of the physical properties and decreases the stability toward the metal anode.[6,7] To overcome these problems, considerable attempts have been made to modify the properties of solid polymer electrolytes, for example, forming networks and copolymers with other functional groups and introducing comb-branch units.[8–10]

On the other hand, ion transport in polyether is closely coupled to the segmental motions of the local chains. With regard to ion transport, it is well known that ionic conductivity occurs in the amorphous phase above the glass transition temperature (T_g), where the transport is induced by the local motion of polyether chain segments, repeatedly creating new coordination complexes into which the ions may then migrate.[11] Therefore, the selection of a proper polymer electrolyte must be based not only on fast ion-transport properties but also on favorable reaction kinetics for enhancement of the segmental motion, creating a dynamic and disordered environment. In this process, the reaction kinetics of reacting monomers is analyzed by differential scanning calorimetry (DSC). DSC is one of techniques that has been widely used to evaluate the cure kinetics such as of amine/epoxy and anhydride/epoxy resins and unsaturated polyester resin systems.[12,13] It is used for the quantitative determination of the fractional conversion and conversion rate during the polymerization in dynamic and isothermal conditions. Here, a dynamic kinetic model was used to study the reaction kinetics of monomers, because the degree of conversion and kinetic parameters are defined by the reaction kinetics. Moreover, understanding the reaction kinetics of the monomer becomes an essential factor for defining both the polymer morphology and the mobility, such as the molecular local motion and the T_g, which plays a critical role in ionic conductivity.

Until now, investigation of polymer electrolytes has long been focused primarily on the enhancement of the ionic conductivity at room temperature via various approaches such as using blends and copolymers, introducing inorganic fillers, and using crosslinked formation and comblike branched networks. However-

Correspondence to: M. Sumita (msumita@o.cc.titech.ac.jp).

Journal of Applied Polymer Science, Vol. 89, 2149–2156 (2003)

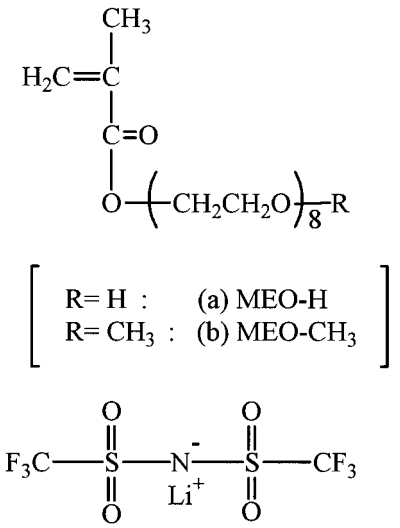

Figure 1 Molecular structures of MEO monomers and Li salt.

,the reaction kinetics of the monomer has received relatively little attention because it was not considered to support the ionic conductivity. In this study, the effects of the reaction kinetics on ion-conductive behavior are discussed on the basis of the ionic conductivity data and structural characterization obtained from DSC and ^{1}H pulse NMR studies.

EXPERIMENTAL

Materials

Two types of oligo(oxyethylene methacrylate) (MEO; NOF Co.) as monomers of the host polymer matrix and lithium bis(trifluoromethane sulfonyl)imide (LiTFSI; Sumitomo 3M) as the salt were used for preparation of electrolyte film. These molecular structures are shown in Figure 1. The LiTFSI was used after drying at 100°C under a vacuum for 24 h.

Preparation of the specimen

The starting homogeneous solutions were obtained from the MEO dissolved in dehydrated methanol with LiTFSI and 1.0 mol % of AIBN. The concentration of LiTFSI was expressed as the molar ratio of Li^+ to the repeating unit of oxyethylene (OE), $r = [Li^+]/[OE] \times 100$, ranging from 1.25 to 10.0 mol %. Upon removal of the solvent, the resulting mixture was dried under a vacuum at 40°C for 24 h and then stored in dry nitrogen gas before preparation of the corresponding specimens. An approximately 1.0-mm-thick free-standing specimen measured by a micrometer was obtained from the dynamic heating process. The four different heating rates, 5, 10, 15, and 20°C/min, were controlled from 30 to 160°C using a temperature controller unit (Chino KP1000) to estimate the effect of the reaction kinetics of the monomer on the ionic conductivity in this system. The prepared films were further dried in the vacuum oven at 40°C for 12 h.

Measurements

Kinetic analysis of the liquid monomer–Li salt mixtures including AIBN were carried out using a DSC-50 thermal analyzer (TA-50WS, Shimadzu) under a nitrogen atmosphere at different heating rates of 5, 10, 15, and 20°C/min from 30 to 160°C. The kinetic parameters such as the maximum heat of reaction, ΔH_{tot}, the degree of conversion, α, and the reaction activation energy, E, were calculated. To determine the T_g of the prepared MEO films, DSC measurements were also taken over a temperature range from −80 to 200°C at a heating rate of 10°C/min.

The ionic conductivity was measured by the complex impedance method using a 4192A LF impedance analyzer (Hewlett–Packard) in the frequency range from 100 to 20 MHz. The temperature was varied from 30 to 100°C at a heating rate of 2.0°C/min. The measurement cell was constructed with a pair of parallel stainless-steel (SUS) plates with a 1.0-mm-thick Teflon spacer. This entire process was carried out in an SUS box filled with dry nitrogen gas.

The spin–spin relaxation time (T_2) was measured under isothermal conditions at 37°C using an MQ20 pulse NMR spectrometer (Bruker Minispec) at 20 MHz. The fading curves of the transverse magnetization were recorded using the Carr–Purcell–Meiboom–Gill (CPMG) impulse sequence[14,15] to obtain information about segmental relaxation of ether side chains and methacrylate main chains. The T_2 decay for the samples was analyzed as a sum of ^{1}H-NMR free-induction decay (FID)-type decays.

RESULTS AND DISCUSSION

Polymerization kinetics

Thermodynamics is concerned with the changes in entropy and energy that accompany a change in a system. It is also very important for an understanding of the effect of the monomer structure on polymerization. Using the Gibbs free energy of a reaction, one can predict the direction in which a chemical change will take place and the amount of energy consumed.[16]

The reaction kinetics of this system based on an oligo(oxyethylene)-type monomer initiated with AIBN can be approached by a mechanism of free-radical polymerization that consists of a sequence of

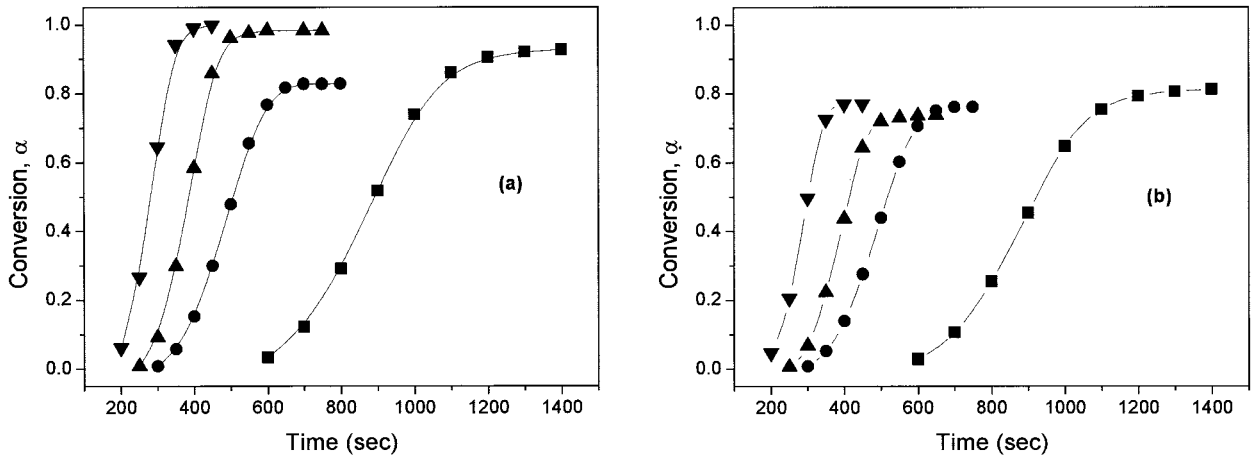

Figure 2 Conversion as a function of reaction time with different heating rates: (a) MEO–H, (b) MEO–CH_3: (■) 5°C; (●) 10°C; (▲) 15°C; (▼) 20°C/min (where r = 2.5 mol %).

steps: initiation, propagation, and termination. The free radicals were produced by thermal decomposition of the initiator. The rate constant of the initiator is given by[17]

$$\frac{d[I]}{dt} = -k_i(T)[I] = -A_i\exp(-E_i/RT)[I] \qquad (1)$$

where $k_i(T)$ is the temperature-dependent kinetic constant of initiation given by an Arrhenius-type equation; $[I]$, the concentration of the initiator; A_i, the collision frequency factor of the initiation step (s^{-1}); E_i, the activation energy of the initiation (kJ/mol); R, the gas constant (kJ mol^{-1} K^{-1}); and T, the absolute temperature (K). Assuming that the exothermic heat generated during the reaction is proportional to the number of double bonds that have reacted in the system, the degree of conversion is defined as

$$\alpha = \frac{[M]_i - [M]}{[M]_i} \qquad (2)$$

where $[M]_i$ is the initial concentration of the monomer, and $[M]$, the concentration at time (t) of the monomer. The rate of a reaction is simply expressed as the rate of the decrease of the reactant or the rate of increase of the products. It is widely accepted that the rate expression for the propagation step of thermal transformation can be expressed as[18]

$$-\frac{1}{[M]_i}\frac{d[M]}{dt} = \frac{d\alpha}{dt} = k_p(T)f(\alpha) = A_p\exp\left(\frac{-E_p}{RT}\right)f(\alpha) \qquad (3)$$

where $k_p(T)$ represents the kinetic constant of propagation; A_p, the collision frequency factor of the propagation step (s^{-1}); $f(\alpha)$, the reaction model of the conversion dependence function; and E_p, the activation energy of the propagation (kJ/mol). In the polymerization reaction, the process is characterized by the effect of the diffusion of the reagents occurring for high conversion, which is due to the increase in viscosity of the reacting matrix (gel effects). By using the gel effects, the termination step can be negligible.[19]

On the other hand, the measurements of DSC may be used for evaluating the reaction process by assuming that the heat evolved during the polymerization reaction is proportional to the overall extent of the reaction given by the relative fraction of the reactants consumed. It is assumed that the maximum conversion is reached when all the double bonds that can react have done so. In this case, the extent of the reaction, α, is proportional to the heat generated and the reaction rate is directly proportional to the rate of heat generation, dH/dt. The resulting relation can be expressed as

$$\alpha = \frac{\Delta H(t)}{\Delta H_{\text{tot}}} \qquad (4)$$

$$\frac{d\alpha}{dt} = \frac{(dH/dt)(t)}{\Delta H_{\text{tot}}} \qquad (5)$$

where $\Delta H(t)$ is the heat of the reaction released at time t (kJ/g), and ΔH_{tot}, the maximum heat of the reaction[20] measured by DSC (kJ/g). The extent of the conversion as a function of time for different heating rates is shown in Figure 2, where the determination of the degrees of conversion according to the time is very useful to define the optimum reaction condition. These plots mean that the rate of the reaction increases with an increasing heating rate. Within the experimental timescale, almost complete conversion was observed in the case of MEO–H except for the case of 10°C/min [Fig. 2(a)]. In the case of 10°C/min, the

behavior could be due to morphological and topological limitations related to comparatively rapid physical changes such as a gelation and a diffusion-controlled step in this system. On the other hand, kinetic curves of MEO–CH_3 revealed the maximum rates of conversion to be around 0.8 [Fig. 2(b)]. This means that the value lower than 1.0 in Figure 2 gives proof of the presence of an unreacted monomer or low molecular weight MEO in the electrolyte. As mentioned previously, the thermodynamic characteristics such as free energy, enthalpy related to interaction, and entropy dependent on the structure are important for an understanding of the effect of the monomer structure on polymerization. It is well known that the negative differences in entropy for polymerization arise from the decreased degrees of freedom for the polymer relative to the monomer.[20] Further, the variations in enthalpy arise from differences in the resonance stabilization of the monomer and polymer and steric differences in the monomers. These results demonstrate the possibility that ionic transport in MEO electrolytes can be controlled by the kinetic rate, which resulted from the morphological structure, the reactivity of the monomers, thermodynamical changes during the reaction process, and kinetic parameters owing to the reaction condition.

Dynamic kinetic analysis procedures

In general, in a polymerization initiated by the thermal decomposition of an initiator, the polymerization rate depends on the ratio of three rate constants, k_i, k_p, k_t, and their temperature dependence is evaluated by combining three separate Arrhenius-type equations as follows[20]:

$$\ln\left[k_p\left(\frac{k_i}{k_t}\right)^{1/2}\right] = \ln\left[A_p\left(\frac{A_i}{A_t}\right)^{1/2}\right] - \left[\frac{E_p + (E_i/2) - (E_t/2)}{RT}\right] \tag{6}$$

As mentioned earlier , the kinetic parameters of the termination step, k_t and A_t, can be negligible due to the gel effect.[19] Actually, the thermodynamic properties of a polymerization relate only to the propagation step. In addition, we also examined the same concentration of the initiator and the measurement condition. Therefore, considering these simplifications and assumptions, eq. (6) can be reduced using the factor of the effective reaction rate constant, k_{eff}, as follows in this system:

$$\ln[k_{\text{eff}}] = \ln[A_{\text{eff}}] - \frac{E_{\text{eff}}}{RT} \tag{7}$$

where A_{eff} is the effective collision frequency factor (s^{-1}), and E_{eff}, the effective reaction activation energy (kJ/mol). Generally, there are a few types of procedures for dynamic kinetic analysis.[21] Among them, to obtain kinetic parameters such as the reaction activation energy, E, and the collision frequency factor, A, the Kissinger evaluation method[22] was performed in this study. Kissinger's method is based on the assumption that the exothermic peak coincides with the maximum reaction rate and is derived based on eqs. (3) and (7) as follows:

$$\frac{d\alpha}{dt} = A_{\text{eff}}(1-\alpha)^n \exp\left(-\frac{E_{\text{eff}}}{RT}\right) \tag{8}$$

where $d\alpha/dt$ is the rate of conversion, and n, the reaction order. Equation (8) can be described in terms of differentiating α and T with respect to the reaction time t; thus:

$$\frac{d}{dt}\left(\frac{d\alpha}{dt}\right) = \frac{d\alpha}{dt}\left[\frac{E_{\text{eff}}\phi}{RT^2} - A_{\text{eff}} n(1-\alpha)^{n-1}\exp\left(-\frac{E_{\text{eff}}}{RT}\right)\right] \tag{9}$$

where ϕ is the linear heating rate. In the case of the maximum reaction rate, eq. (9) becomes zero and can be written

$$\frac{E_{\text{eff}}\phi}{RT_p^2} = A_{\text{eff}} n(1-\alpha)^{n-1}\exp\left(-\frac{E_{\text{eff}}}{RT}\right) \tag{10}$$

where T_p refers to temperature at the peak of the DSC curve of the corresponding experiment. It is generally accepted that the term $n(1-\alpha)^{n-1}$ is independent of the heating rate and the value is close to unity as 1. Then, the simplified form of the Kissinger expression is given by

$$\frac{E_{\text{eff}}\phi}{RT_p^2} = A_{\text{eff}}\exp\left(-\frac{E_{\text{eff}}}{RT_p}\right) \tag{11}$$

By linearizing and rearranging the above equation, the following equation results:

$$\ln\left(\frac{\phi}{T_p^2}\right) = \ln\left(\frac{A_{\text{eff}}R}{E_{\text{eff}}}\right) - \left(\frac{E_{\text{eff}}}{RT_p}\right) \tag{12}$$

According to eq. (12), the effective reaction activation energy and the collision frequency rate can be obtained from the slope and from the intercept of the linear relationship $\ln[\phi/{T_p}^2]$ against ${T_p}^{-;1}$, respectively.

Figure 3 shows the exothermic DSC thermograms of the MEO electrolytes for various heating rates. The

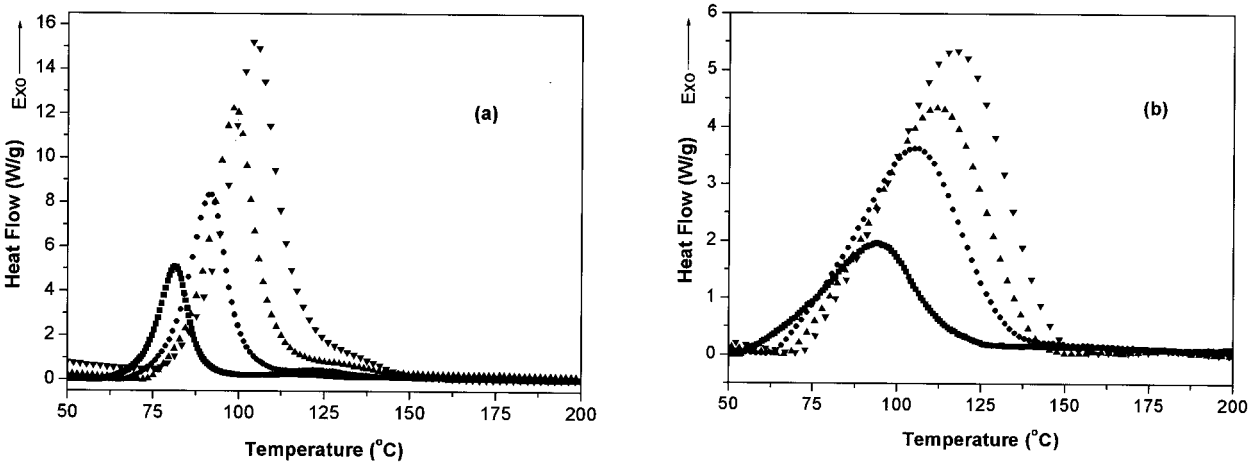

Figure 3 Dynamic DSC thermograms of the electrolytes containing LiTFSI with AIBN for various heating rates: (a) MEO–H, (b) MEO–CH_3: (■) 5°C; (●) 10°C; (▲) 15°C; (▼) 20°C/min (where r = 2.5 mol %).

exothermic nature of polymerization is caused by the exothermic conversion of π-bonds in monomer molecules into σ-bonds in the polymer. In these thermograms, the peak temperature (T_p) represents the maximum reaction rate increase with an increasing heating rate. The quantity of the peak shift due to the increase of heating rate depends on the activation energy of the reaction.

Figure 4 shows the effective reaction activation energy calculated from the slope using eq. (12). It reveals that the slope of $\ln[\phi/T_p^2]$ against T_p^{-1} is influenced by the amount of Li salt and the structure of the monomer. Consequently, the activation energy increased with the salt content and the values of MEO—CH_3 were higher than those of MEO—H. This behavior of the collision frequency rates also showed the same trend with the results of the activation energy as a function of the Li salt fraction; however, they revealed a reciprocal trend with the type of the monomer as shown in Figure 5. These results indicated that the reaction mechanism was likely to be changed by the presence of LiTFSI and the type of the monomer in the electrolyte. As a result, a steric effect of the terminal group is probably the more important factor in determining the value of k_{eff}. Therefore, the more hindered monomer, MEO–CH_3, has lower k_{eff} and A_{eff} values than has the less hindered MEO–H, probably owing to a large decrease in the entropy on the polymerization and showed increased reaction activation energy in this system.

Effect of reaction kinetics on the ionic conductivity

The salt concentration dependence of the ionic conductivity for the PMEO electrolyte is shown in Figure

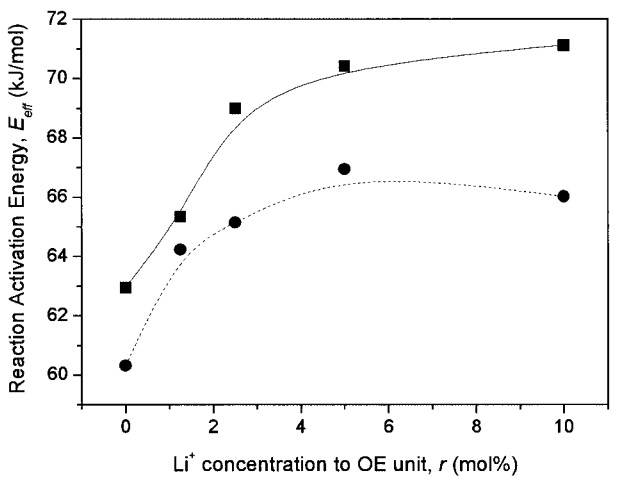

Figure 4 Effective reaction activation energies obtained by Kissinger method with salt fraction: (●) MEO–OH; (■) MEO–CH_3.

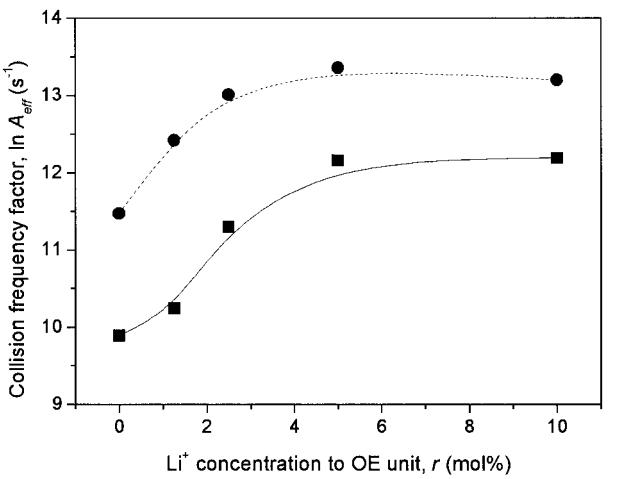

Figure 5 Effective collision frequency rate as a function of salt fraction: (●) MEO–H; (■) MEO–CH_3.

6. With the salt fraction increase, the enhanced amount of salt dissociation produces more free ions, which accelerate the ionic mobility that assists the ionic conductivity. It is also observed that for the addition of salt of more than $r = 5$ mol % there is a decrease in the ionic conductivity in the case of PMEO–H, which may be due to the reduction in the segmental motion of the ether chains. Above a critical value of the Li salt concentration, the salt can perform kinetically, inhibiting the local relaxation and segmental motion of the polymer chains to allow ion transport. These results show good agreement with those of the reaction kinetics as shown in Figures 4 and 5. In this system, below a Li salt concentration of $r = 5$ mol %, it is supposed to play an accelerating effect. Meanwhile, ion association occurs with the Li compounds because of the small size of the Li ions and their possessing more low-energy orbitals than electrons above a critical value. In the propagation step, the ion aggregation is important since the associated species are far less reactive than are the unassociated species and retards the collision frequency rate. The phenomenon is also affected by steric hindrances with the type of terminal group.

For the purpose of investigating the effect of the reaction kinetics on the ionic conductivity systematically, the electrolytes were prepared by different reaction conditions. The evaluated results such as T_g and ionic conductivity are summarized in Table I. From these results, it is found that the influence of the reaction-heating rate on the T_g is related to local segmental mobility. As the T_g decreases, the amorphous phase or the less ordered regions become more flexible, resulting in increased segmental motion of the MEO side chains, which reflects the enhancement of the ionic conductivity. It is clearly related to the results of the conversion in Figure 2. As previously stated, a

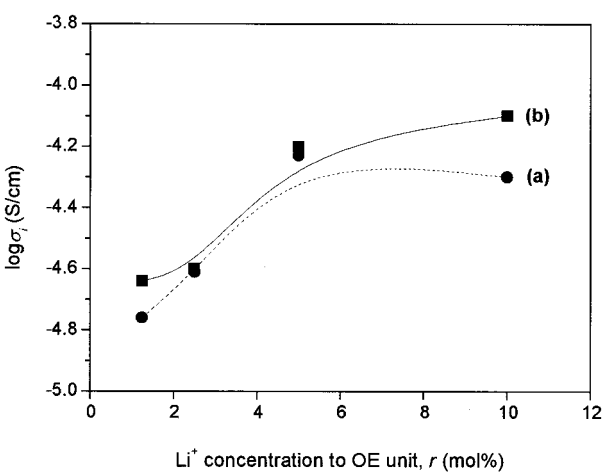

Figure 6 Salt fraction dependence of the ionic conductivity for (a) PMEO–H and (b) PMEO–CH_3 at 40°C.

TABLE I
Influence of the Reaction Heating Rate on T_g and Ionic Conductivity (r = 2.5 mol %)

Reaction heating rate (°C/min)	T_g (°C)		log σ_i (S/cm at 40°C)	
	PMEO–H	PMEO–CH_3	PMEO–H	PMEO–CH_3
5	−60	−63	−4.97	−4.66
10	−62	−65	−4.53	−4.56
15	−58	−66	−4.86	−4.39
20	−56	−65	−5.00	−4.53

low conversion that resulted from the presence of unreacted monomer or oligomer decreases the T_g and increases the degree of randomness for the MEO network. It plays an important role in enhancing the ion transport. In this table, the nonlinearity of the ionic conductivity indicates that the ion transport in PMEO is dependent on the polymer segmental motion. Since the electrolytes are amorphous polymers, the results may be more effectively analyzed by the empirical Vogel–Tamman–Fulcher (VTF) equation originally used to characterize the viscoelastic properties of polymer systems[23–25]:

$$\sigma_i = A_c T^{-1/2} \exp\left[-\frac{E_a}{T - T_0}\right] \tag{13}$$

where A_c is a preexponential factor that is associated with the number of charge carriers (S cm^{-1} K$^{-1/2}$); E_a, the conduction activation energy (kJ/mol); and T_0, the quasi-equilibrium ideal T_g.[26] The VTF equation is based on the free-volume model and E_a is related to the activation energy of the ion transport associated with the structural entropy of the polymer chains and obtained from the slope of Figure 7. As calculated results, the electrolytes prepared by the reaction heating rate of 10°C/min for MEO–H and 15°C/min for MEO–CH_3 showed the maximum value of A_c and exhibited a minimum E_a for the free-volume redistribution, as summarized in Table II. As the E_a decreases, the dissociation of salts is promoted, which means that free ions can be easily prepared from the ion pairs or aggregate ions, resulting in increased ionic conductivity.

CPMG ^{1}H pulse NMR analysis

Transport of a cation in a polymer electrolyte is controlled by the dynamic relaxation modes of the host polymer. With regard to segmental motion, it is known that the relaxation time is dynamic information for characterizing the backbone and side-chain motions. Figure 8 shows the effect of the reaction heating rate on the spin–spin relaxation time, T_2. The

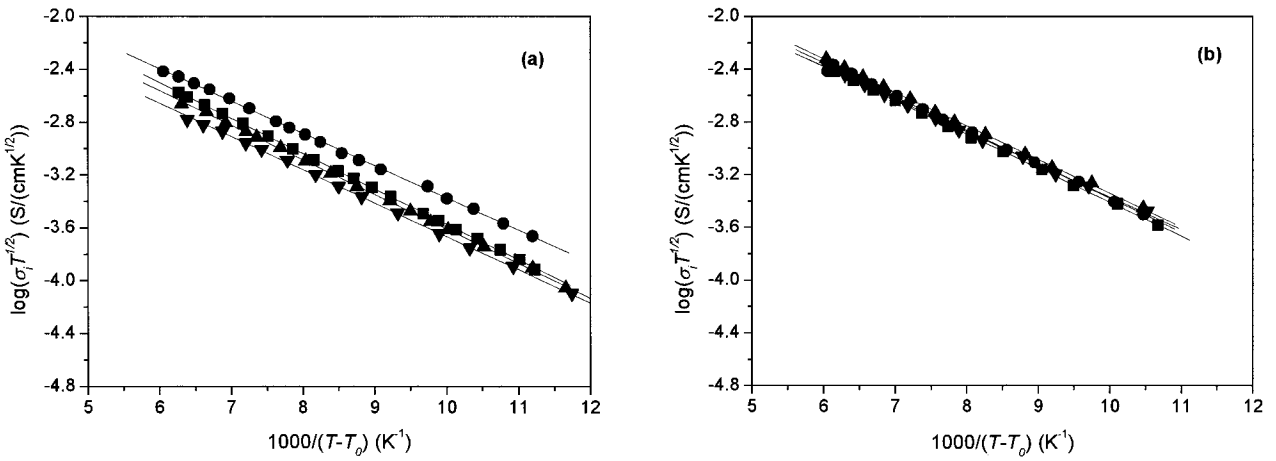

Figure 7 Reaction heating rate dependence of VTF plots for (a) PMEO–H, (b) PMEO–CH_3: (■) 5°C; (●) 10°C; (▲) 15°C; (▼) 20°C/min (where r = 2.5 mol %).

T_2 values are determined from the slope of the plot of ln M against time t,[27] where M is the amplitude of the FID signal. A quantitative analysis of the decay shape is not always straightforward due to the complex origin of the relaxation function itself and the structural heterogeneity of the chain segment. In this system, the T_2 decays are represented by the sum of the three discrete relaxation components that suggest heterogeneity of the chain motion, a long T_{2a} component corresponding to the mobile region, an intermediate T_{2b} component of the interfacial region among the chains, and a short T_{2c} component related to the immobile main chain. The most mobile components based on T_{2a} are those elements which are contained in the free side chains, not from the crosslink structures. These results provide useful information about the relationship between the molecular mobility originated from the reaction condition and ionic conductivity affected by the segmental motion. In this work, the reaction heating rate of 10°C/min of MEO–H and 15°C/min of MEO–CH_3 showed the highest value of T_{2a}. These also show good agreement with the results of σ_i at 40°C in Table I. Consequently, the low conversion enhances the degree of freedom for PMEO electrolytes and provides high flexibility and a high free volume to increase the segmental motion that resulted in high ionic conductivity.

TABLE II
Influence of the Reaction Heating Rate on the Constant Related to the Number of Charge Carriers, A_c, and the Conduction Activation Energy, E_a, Using VTF Plots (r = 2.5 mol %)

Reaction heating rate (°C/min)	A_c (S cm^{-1}K$^{-1/2}$)		E_a (kJ/mol)	
	PMEO–H	PMEO–CH_3	PMEO–H	PMEO–CH_3
5	0.13	0.14	2.18	2.16
10	0.15	0.15	2.08	2.02
15	0.10	0.16	2.22	1.95
20	0.07	0.13	2.25	2.10

CONCLUSIONS

Solid polymer electrolytes based on PMEO with LiTFSI were prepared by different reaction conditions, and the effect of the reaction kinetics on the ion-conductive behavior was evaluated. The reaction condition affected not only the kinetics but also the ionic conductivity of the polyether electrolytes.

As experimental results, the kinetic parameters were not constant and showed a dependence upon the heating rate. Especially, the reaction activation energy was in concordance with the values of the degree of conversion and was affected by the concentration of salt. These tendencies were also in agreement with the results of the impedance analy-

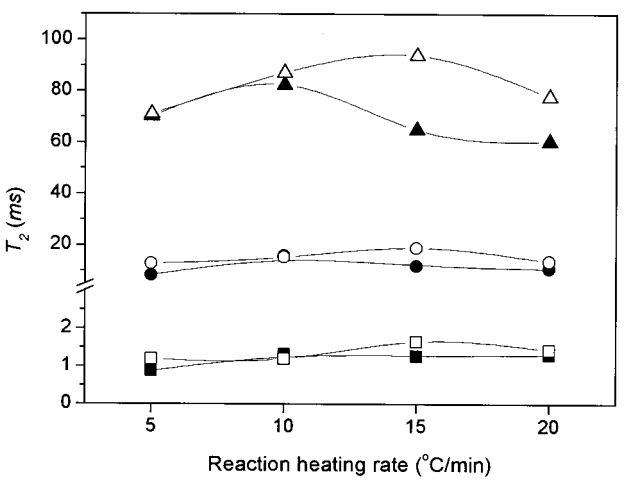

Figure 8 Reaction heating rate dependence of T_2 by ^{1}H pulse NMR: (a) (closed) PMEO–H, (b) (open) PMEO–CH_3: (▲,△) T_{2a}; (●,○) T_{2b}; (■,□) T_{2c} (where r = 2.5 mol %).

sis. Consequently, it was noted that the correlation between the reaction kinetics and the ionic conductivity was preserved for the segmental motions of the ether chains and the steric effects results from the terminal group of the monomer. From this study, it was revealed that there was an optimum rate of the reaction to form polyether electrolytes for high ionic conductivity.

References

1. Fenton, D. E.; Parker, J. M.; Wright, P. V. Polymer 1973, 14, 589.
2. Scrosati, B. In Polymer Electrolyte Reviews; MacCallum, J. R.; Vincent, C. A., Eds.; Elsevier: New York, 1989.
3. Schantz, S.; Torrel, L. M.; Sterens, J. R. J Chem Phys 1991, 94, 6862.
4. Solid State Electrochemistry; Shriver, D. F.; Bruce, P. G., Eds.; Cambridge University: Cambridge, 1995.
5. Mani, T.; Stevens, J. R. Polymer 1992, 33, 834.
6. Bohnke, O.; Rousselot, C.; Gillet, P. A.; Trouche, C. J Electrochem Soc 1992, 139, 1862.
7. Croce, F.; Brown, S. D.; Greenbaum, S. G.; Slane, S. M.; Salomon, M. Chem Mater 1993, 5, 1268.
8. Appetecchi, G. B.; Croce, F.; Scrosati, B. Electrochim Acta 1995, 40, 991.
9. Rajendran, S.; Uma, T. Bull Mater Sci 2000, 23, 31.
10. Choi, B. K.; Kim, Y. W.; Shiv, K. H. J Power Sources 1997, 68, 357.
11. Druger, S. D.; Ratner, M. A.; Nitzan, A. Solid State Ion 1983, 9/10, 1115.
12. Patel, M. B.; Patel, R. G.; Patel, V. S. Thermochim Acta 1988, 129, 277.
13. Park, S. J.; Kwak, G. H.; Sumita, M.; Lee, J. R. Polym Eng Sci 2000, 40, 2569.
14. Carr, Y. H.; Purcell, E. M. Phys Rev 1954, 94, 630.
15. Meiboom, G.; Gill, D. Rev Sci Instr 1958, 29, 588.
16. Sastri, S. B.; Keller, T. M.; Jones, K. M.; Armistead, J. P. Macromolecules 1993, 8, 6171.
17. Stevenson, J. F. Polym Eng Sci 1986, 26, 746.
18. Han, C. D.; Le, D. J. Appl Polym Sci 1987, 33, 2859.
19. Balke, S. T.; Hamielec, A. E. J Appl Polym Sci 1973, 17, 905.
20. Principles of Polymerization; Odian, G., Ed.; Wiley: New York, 1991; Chapter 3.
21. Miranda, M. I. G.; Tomedi, C.; Bica, C. I. D.; Samios, D. Polymer 1997, 38, 1017.
22. Kissinger, H. E. Anal Chem 1957, 29, 1702.
23. Ratner, M. A.; Shriver, D. F. Chem Rev 1988, 88, 109.
24. Vogel, H. Phys Z 1921, 22, 645.
25. Tammann, V. G.; Hesse, H. Z. Anorg Allg Chem 1926, 19, 245.
26. Fulcher, G. S. J Am Ceram 1925, 8, 339.
27. Zhou, G.; Khan, I. M.; Smid, J. Macromolecules 1993, 26, 2202.